Magnetic Resonance Imaging of Temperature Changes using TmDOTMA$^-$

S. K. Pakin[1], S. K. Hekmatyar[1], A. M. Babsky[1], P. N. Hopewell[1], N. Bansal[1]
[1]Radiology, Indiana University, Indianapolis, Indiana, United States

Introduction

Magnetic Resonance (MR) temperature monitoring has many direct uses in diagnosis and therapy because tissue temperature and metabolism/physiology are closely interrelated. These uses include aiding in the use of hyperthermia (HT) for treatment of cancer, detection and localization of tumors, diagnosing metabolic abnormalities, and studying muscle exercise and recovery. We have developed noninvasive MR thermometers based on the temperature dependence of hyperfine shifted ^{1}H signals of paramagnetic lanthanide complexes of DOTA^{4-} and DOTMA^{4-} [1]. The temperature dependence of chemical shifts of the ^{1}H resonance from the methyl group of TmDOTMA$^-$ (C_T = 0.586 ppm/^{o}C) is ~60 times more sensitive than water and insensitive to the concentration of the paramagnetic complex, pH, Ca^{2+}, and the presence of plasma macromolecules. In this report, we demonstrate and validate the capability of imaging temperature with sub-degree resolution with TmDOTMA$^-$ in phantoms and show the feasibility of imaging the complex in animals.

Methods

NMR experiments on phantoms were performed on a Varian 9.4 T, 89-mm vertical bore system. The capability of obtaining higher SNR with TmDOTMA$^-$ compared to TmDOTA$^-$ was shown using two concentric NMR tubes. The inner 10-mm tube was filled with tap water, and the outer 20-mm tube was filled with 0.5 or 1.0 mM TmDOTA$^-$ or TmDOTMA$^-$. Transaxial images were acquired using a gradient-echo (GE) sequence without slice selection (TR=16.5 ms, TE=1.3 ms, data grid=32x32, FOV=32x32 mm). Weighted signal summation (WSS) was used to increase the SNR [2]. An average of 64 transients were collected per phase-encoding step. The CHESS technique was used to suppress the strong water signal.

To demonstrate the feasibility of mapping temperature changes with TmDOTMA$^-$, a series of pulse-acquire spectra and spin-echo (SE) projection images (TR=19 ms, TE=3.5 ms, data grid=32x32, FOV=32x32 mm, no slice selection, WSS with 64 average transients per phase-encoding step, CHESS water suppression) of a 20-mm NMR tube containing 4 mM TmDOTMA$^-$ were collected in an interleaved manner. An excess delay (τ) during the second half of the echo time was included in the spin-echo imaging sequence. The total imaging time was 42 s. During acquisition, the temperature of the phantom increased due to RF induction.

To validate the temperature mapping, the imaging experiments were repeated using four fiber optic probes (FOPs) in a 20-mm MR tube containing 1 mM TmDOTMA$^-$. A series of 3D axial images of TmDOTMA$^-$ were acquired using a SE sequence with CHESS (TR = 16.5 ms, TE = 2.7 ms, data matrix = 32x32x8 zero-filled to 64x64x8, and FOV = 32x32x64 mm). A 3D axial GE image of water (TR = 50 ms, TE = 1.3 ms, and data matrix = 64x64x32) was acquired to locate the position of the FOPs. After collecting the images, the coordinates of each temperature probe were found using the water image, and the corresponding voxels in the TmDOTMA$^-$ image were located. The temperature changes at those locations were detected using the average phase accumulation in 7x7x2 pixels around the FOPs.

To demonstrate the feasibility of imaging TmDOTMA$^-$ *in vivo*, projection images of a normal Fisher rat were obtained using a Varian 9.4 T, 31-cm horizontal bore system. A vial containing 4 mM TmDOTMA$^-$ was placed at the side of the rat as a reference. 3D coronal images of TmDOTMA$^-$ were collected using a spin-echo sequence (TR=16 ms, TE=3.4 ms, data grid=64x32x8, FOV=12x5x5 cm, WSS with 43 average transients, CHESS). The total imaging time was 5 min. A high-resolution 3D GE ^{1}H water image (TR=10 ms, TE=1.6 ms, data grid=256x128x32, FOV=12x5x5 cm) was obtained for anatomical comparison.

Results and Discussion

The SNR in 0.5 mM and 1.0 mM TmDOTMA$^-$ images were 13.2 and 26.9, respectively, compared to 3.4 and 6.7 in 0.5 and 1.0mM TmDOTA$^-$ images, respectively. TmDOTMA$^-$ resulted in ~4 times better SNR compared to TmDOTA$^-$, mainly because the former contains three times more protons and has a longer T_2.

Some of the images of temperature changes during the heating experiment are displayed in Figure 1. The images clearly show heterogeneity in the temperature changes during heating. A regression analysis between the values of temperature changes obtained by the phase images (ΔT_i) collected with τ=200 and the simple spectroscopy method (ΔT_s) had a correlation coefficient (R^2) of 0.99 and a regression line of ΔT_i=0.966*ΔT_s-0.1338. A plot of the regional temperatures from the fiber optic probes versus the temperature calculated from the phase-shift near each probe in the 3D image of TmDOTMA$^-$ also gave an excellent fit (R^2 =0.98). These data show that TmDOTMA$^-$ can be employed to map heterogeneity in temperature changes with sub-degree accuracy by using the phase imaging sequence.

Figure 2 shows a set of representative coronal slices from the *in vivo* 3D images of methyl signal from TmDOTMA$^-$ before and after injection of TmDOTMA$^-$ in a rat and a high-resolution water image. The image collected before TmDOTMA$^-$ injection shows signal only from the vial containing 4 mM TmDOTMA$^-$, indicating efficient supression of the strong water signal. The image obtained after TmDOTMA$^-$ injection shows a relatively homogeneous distribution of TmDOTMA$^-$ throughout the animal's body. In a separate experiment, we did not observe any TmDOTMA$^-$ signal from the brain, which suggests that similar to various MRI contrast agents, TmDOTMA$^-$ does not cross the blood-brain barrier.

Conclusion:

We have demonstrated the capability of mapping sub-degree changes in temperature using TmDOTMA$^-$ as a MR thermometer. We have also shown the fesability of obtaining ^{1}H images of TmDOTMA$^-$ in intact animals.

References:

1. Hekmatyar SK, Poptani H, Babsky A, Leeper DB, Bansal N, *Int. J. Hyperthermia*, 18(3): 165-179, 2002
2. Bansal N, Seshan V, *Jour. Magn. Res. Img.*, 5(6): 761-767 1995

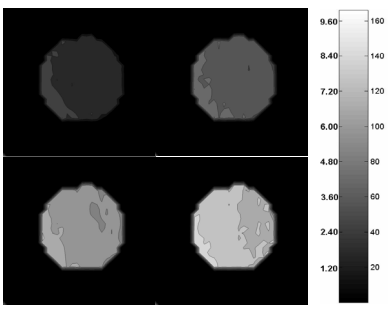

Fig 1: Four snapshots of temperature changes during the heating of phantom.

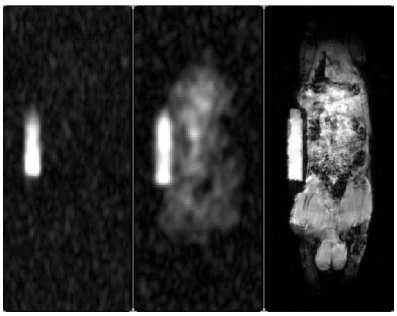

Fig 2: *In vivo* ^{1}H MRI of TmDOTMA$^-$ before (left) and after (middle) injection and a water ^{1}H MRI (right).